

Elastic Scattering of 14-Mev Neutrons from Beryllium and Carbon*

M. P. NAKADA, J. D. ANDERSON, C. C. GARDNER, AND C. WONG
University of California Radiation Laboratory, Livermore, California

(Received February 24, 1958)

The angular distributions of elastically scattered 14-Mev (nominal energy) neutrons have been measured for beryllium and carbon from 20° to 140° . Ring geometry, time-of-flight techniques, and relatively low detector biases were used. A comparison with optical-model calculations by Bjorklund and Fernbach indicates that the parameters that fit the medium and heavy elements do not yield satisfactory fits for beryllium and carbon.

INTRODUCTION

OPTICAL-MODEL calculations by Bjorklund and Fernbach¹ have yielded excellent fits to the existing 14-Mev scattering data for elements heavier than aluminum. For elements lighter than Al, the predicted angular distributions might show progressively worse fits as A decreases, since the applicability of the optical model to light nuclei is questionable. This experiment was undertaken to compare the Be and C angular distributions with the predictions of reference 1.

Because of the large elastic energy degradation, standard biased detector techniques² prove very difficult. For example, to look at elastically scattered neutrons from Be at 90° the detector bias must be below 11 Mev. At 30° , however, this bias would then yield a detectable number of inelastic counts from the

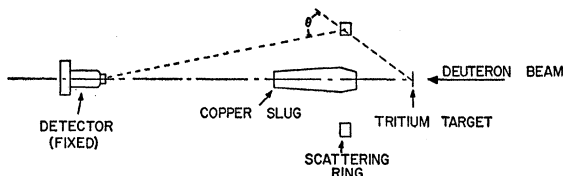


FIG. 1. Schematic diagram of the experimental setup. The angle of scattering is denoted by θ . The scattering rings had a mean radius of 14 cm and were either square or rectangular in cross section.

TABLE I. Variations made in the geometry and parameters.

Element	Angular range (deg)	Ring cross section (in. \times in.)	Detector-to-target distance (in.)	Detector	Detector bias (Mev)
Be	20-80	1 \times 1	135.5	Plastic ^a	3.8
	50-140	1 \times 1	120	Plastic	3.8
C	20-80	1 \times 1	135.5	Plastic	3.8
	20-80	1 \times 2	135.5	Plastic	3.8
	30-140	1 \times 2	81	Stilbene ^b	1.7
	30-140	1 \times 2	81	Stilbene	1.1 ^c
	30-140	2 \times 2	81	Stilbene	1.7

^a The plastic scintillator was 2 in. in diameter by $2\frac{1}{4}$ in. thick.

^b The stilbene detector was surrounded by lead and paraffin. Stilbene scintillator was $1\frac{1}{2}$ in. in diameter by 0.8 in. thick.

^c Biased at one-half of the 0.511-Mev gamma-ray Compton edge.

* Work performed under the auspices of the U. S. Atomic Energy Commission.

¹ F. Bjorklund and S. Fernbach, University of California Radiation Laboratory Report UCRL-4926T, 1957 (unpublished).

² J. O. Elliot, Phys. Rev. **101**, 684 (1956).

2.4-Mev level in Be. Thus many different detector biases would be necessary to cover the entire range of scattering angles. By time separating the elastic from the inelastic neutrons, a single, and at the same time a relatively low, detector bias could be employed. A low detector bias is desirable for increased stability, for greater efficiency, and for smaller changes of detector efficiency with scattering angle. Since gamma rays from inelastic scattering are also time separated from elastic neutrons, a large and efficient scintillator can be used.

EXPERIMENTAL DETAILS

Figure 1 is a schematic drawing of the experimental setup. The swept and bunched³ 0.5-Mev deuteron beam of the Cockcroft-Walton accelerator strikes a tritium-loaded target and produces short bursts of 14-Mev neutrons. Some of these neutrons elastically scatter from the ring at an angle θ and are detected in a plastic or stilbene scintillator. A 30-inch copper absorber shields the detector from the source neutrons. The geometry and parameters were varied (see Table I) in an effort

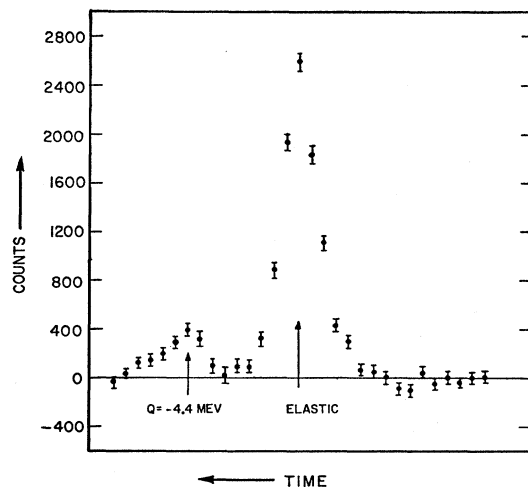


FIG. 2. Time spectrum for carbon at a scattering angle of 25° . The time scale is 1 μ sec per channel, and increasing flight time is towards the left. The target-to-detector distance was 135.5 in., and the detector bias was 3.8 Mev.

³ Ashby, Harris, Klein, and Nakada, University of California Radiation Laboratory Report UCRL-4641, September, 1955 (unpublished).

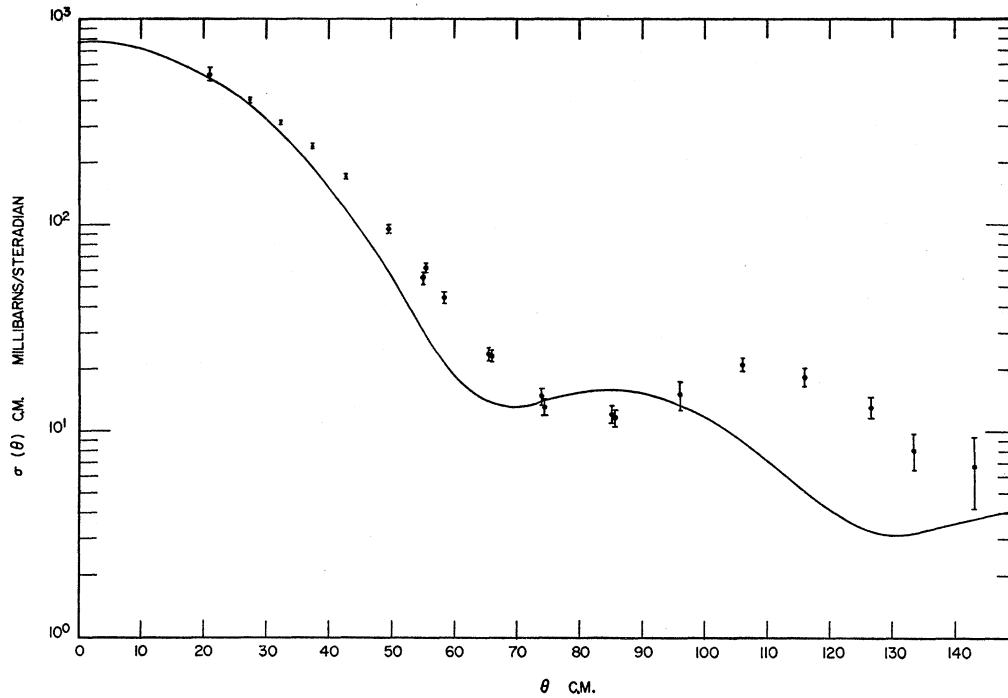


FIG. 3. The Be angular distribution in the center-of-mass system. Solid curve is the prediction of reference 1.

to check on systematic errors. The angle of scattering, θ , is varied by moving the ring scatterer with respect to the target. This results in a change of the incident neutron energy with scattering angle. At $\theta=20^\circ$, the mean incident neutron energy is 14.7 Mev; at 90° , 14.1 Mev; and at 140° , 13.6 Mev. For convenience, 14 Mev is quoted as the nominal neutron energy.

The detector biases were set with reference to the Compton edges of the 0.511- and 1.275-Mev gamma rays from a Na^{22} source. After setting the biases, the detector efficiencies were measured at 14.7 Mev by sampling direct neutrons at 0° . The energy dependence of the efficiencies was measured by scattering from polyethylene (n - p differential scattering). The proton

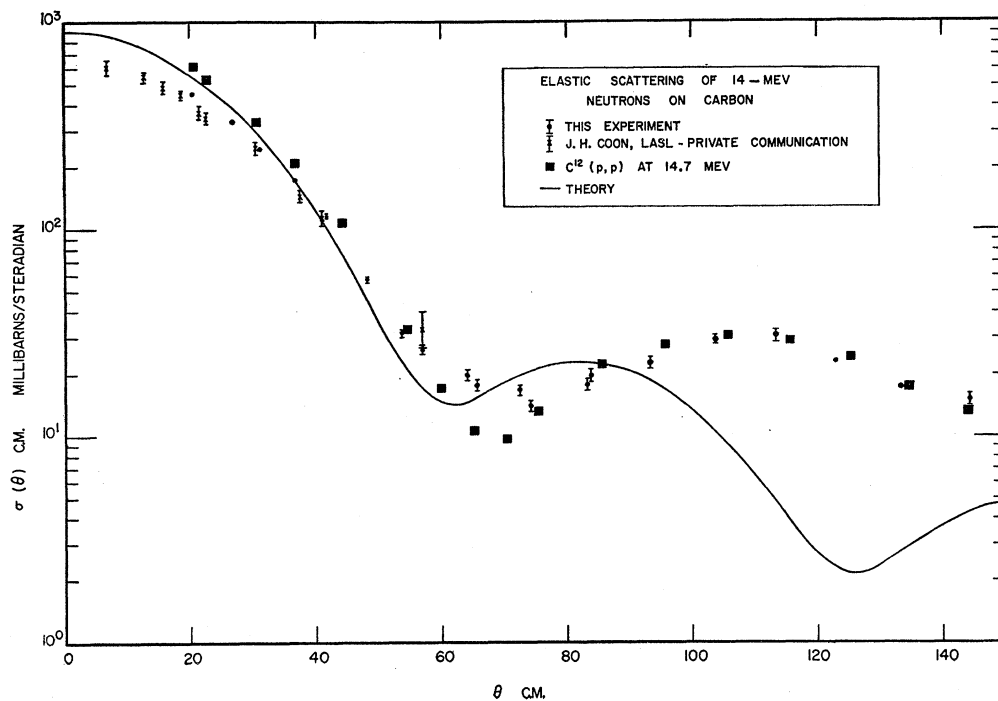


FIG. 4. The carbon angular distribution in the center-of-mass system. Solid curve is the prediction of reference 1. Also plotted are the neutron scattering data of Coon *et al.* (reference 8) and the proton scattering data of Peelle. Where applicable, size of symbols indicates statistics.

recoil bias energies associated with the 0.511- and 1.275-Mev Compton edges were determined to be 1.7 and 3.8 Mev, respectively. These bias energies are in reasonable agreement with those obtained from electron-to-proton pulse-height ratios.⁴ The measured energy dependence agrees well with calculations for all bias settings. For a description of the time-of-flight electronics and monitoring, the reader is referred to a previous paper.⁵

RESULTS

A typical time spectrum for C at 25° is shown in Fig. 2. The elastically scattered neutrons are clearly separated from the first-level inelastically scattered neutrons. The full width at half-maximum of the elastically-scattered-neutron peak is about 4 μ sec, which is a measure of the resolution of our time-of-flight system.

After making Monte Carlo corrections for multiple scattering, absorption, and angular resolution due to finite ring size, the cross sections obtained from the different size rings agreed with each other within statistics. The final combined results are shown in Figs. 3 and 4. The Monte Carlo calculations do not correct for finite size of the detector, since a point source and detector were assumed for the calculations. The residual angular resolution due to detector size is less than $\pm 1^\circ$.

Upon using a reasonable extrapolation for angles less than 20° (see Fig. 5 for Be), the integrated elastic cross sections are: Be, 0.94 ± 0.05 barn; C, 0.79 ± 0.05 barn. Since for the total cross sections $\sigma_T(\text{Be}) = 1.51 \pm 0.03$ barns and $\sigma_T(\text{C}) = 1.32 \pm 0.03$ barns,⁶ this implies $\sigma_{ne}(\text{Be}) = 0.57 \pm 0.06$ barn and $\sigma_{ne}(\text{C}) = 0.53 \pm 0.06$ barn for the nonelastic cross sections. These latter values agree within statistics with the nonelastic measurements of Ball, Booth, and MacGregor⁷: $\sigma_{ne}(\text{Be}) = 0.49 \pm 0.02$ barn and $\sigma_{ne}(\text{C}) = 0.56 \pm 0.02$ barn.

DISCUSSION

The predictions of reference 1 for Be and C are shown in Figs. 3 and 4. The shapes and magnitudes are predicted correctly, but the minima and maxima occur at the wrong places. Possible explanations for the poor fits are:

1. The assumed dependence of $r = r_0 A^{\frac{1}{3}}$ may not be applicable.

2. For Be and C at 14 Mev there may be an appreciable contribution from compound elastic scattering.

Further calculations are being done by Bjorklund and Fernbach in an effort to fit the Be and C angular distributions.

⁴ C. J. Taylor *et al.*, Phys. Rev. **84**, 1041 (1951).

⁵ Anderson, Gardner, Nakada, and Wong, Phys. Rev. **110**, 160 (1958).

⁶ Bratenahl, Peterson, and Stoering, Phys. Rev. **110**, 927 (1958).

⁷ Ball, Booth, and MacGregor, Phys. Rev. **108**, 726 (1957).

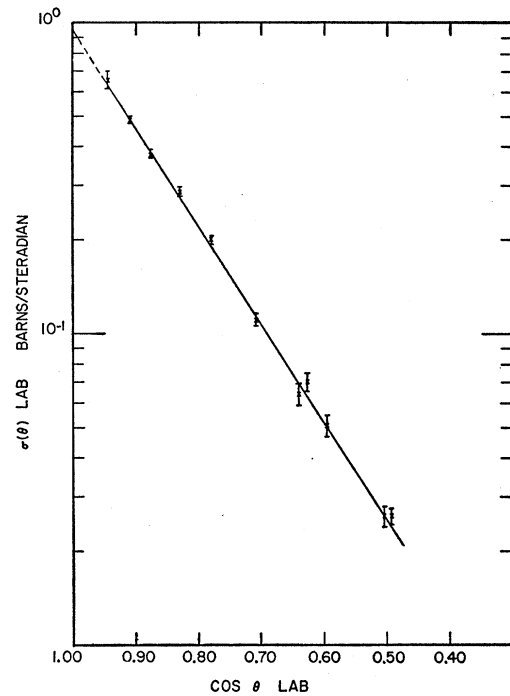


Fig. 5. A semilog plot of $\sigma(\theta)$ versus $\cos\theta$ for Be. The dashed portion represents an extrapolation to angles less than 20°.

The measurements on carbon by Coon *et al.*⁸ are shown plotted on Fig. 4. Our measurements at the forward angles tend to be systematically higher, and may be attributed to the fact that the incident-neutron energy averages near 14.6 Mev, slightly higher than Coon *et al.*'s value of 14.1 Mev. This explanation is plausible since the carbon total cross section is rising between 14.1 and 14.6 Mev.⁹

It is also interesting to compare neutron and proton scattering data for carbon. In Fig. 4 are plotted the proton elastic scattering data of Peelle¹⁰ for an incident energy of 14.7 Mev. The remarkable agreement over most of the angular range indicates that the neutron and proton see approximately the same nuclear potential.

ACKNOWLEDGMENTS

The authors are grateful to F. Bjorklund and S. Fernbach for many discussions concerning their optical model, to M. Mansigh and to J. Hudson for programing and running the Monte Carlo problem on the Univac, and to J. M. Peterson for continued interest and encouragement during the course of the experiment.

⁸ Coon, Davis, Felthaus, and Nicodemus (private communication from J. H. Coon); Phys. Rev. (to be published).

⁹ J. P. Conner, Bull. Am. Phys. Soc. Ser. II, **2**, 267 (1957).

¹⁰ R. W. Peelle, Phys. Rev. **105**, 1311 (1957).